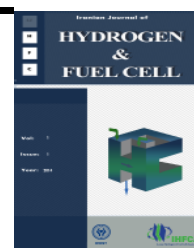


Iranian Journal of Hydrogen & Fuel Cell

IJHFC

Journal homepage://ijhfc.irost.ir



## Electrophoretic deposition of $\text{MnCr}_2\text{O}_4$ coating for solid oxide fuel cell metallic interconnects

Reza Irankhah<sup>\*1</sup>, Babak Raesi Dehkordi<sup>1</sup>, Amir Maghsoudipour<sup>1</sup>,  
Abdullah Irankhah<sup>2</sup>

<sup>1,\*</sup> Department of Ceramic, Materials and Energy Research Center, Tehran, 14155-4777, Iran

<sup>2</sup> Hydrogen and Fuel Cell Research Lab, Chemical Engineering Department, University of Kashan, Kashan, 87317-51167, Iran

### Article Information

Article History:

Received:

2 August 2013

Received in revised form:

4 October 2013

Accepted:

17 January 2014

### Keywords

Solid Oxide Fuel Cell

Interconnect

Spinel

Electrophoretic Deposition

Oxidation Resistance

### Abstract

In the present study, Mn-Cr spinel powder was synthesized through a solid state reaction. In the next step, the electrophoretic deposition (EPD) method was used to apply the  $\text{MnCr}_2\text{O}_4$  spinel, as an oxidation-resistant layer on SUS 430 stainless steel with a potential of 300 V/cm. The coated and uncoated samples were then pre-sintered in air at 900°C for 3h, followed by cyclic oxidation at 800°C for 500h.

In order to study the effect of reducing pre-sintering atmosphere on oxidation resistance, the coated specimen was pre-sintered in 5%  $\text{H}_2/\text{Ar}$  at 900°C for 3h, followed by cyclic oxidation at 800°C for 500h. The results of the oxidation resistance tests revealed that the  $\text{MnCr}_2\text{O}_4$  spinel coating improved the oxidation resistance of the uncoated sample; and also, the oxidation rate constant ( $K_p$ ) for pre-sintered coating in 5%  $\text{H}_2/\text{Ar}$  was nearly 14 times smaller than that of the one pre-sintered in air.

## 1. Introduction

Solid oxide fuel cells (SOFCs), as new electric power generating systems, consist of two electrodes (anode and cathode) separated by the electrolyte [1-3]. The special feature of this generator is its ability to attain almost theoretical energy efficiency by converting chemical energy of the fuel oxidation reaction directly into electrical energy [4]. Moreover, SOFC enables ecological combustion of various types of fuels, e.g. natural

gas, methanol or coal gas without harmful emissions [4]. The interconnect of a solid oxide fuel cell (SOFC) stacks electrically and physically connects the anode of one fuel cell to the cathode of the adjacent fuel cell in the stack (Figure 1). The aim is to connect cells in series, so that the electricity generated by all cells are added up together combined. SOFC interconnects are exposed to both the oxidizing and reducing sides of the cell at high temperatures [5]. For high temperature applications (around 1000°C), ceramic

\*Corresponding author. Email: r.irankhah@yahoo.com  
Tel: +989159042349

interconnects made of lanthanum–chromium oxides doped with strontium show high electrical conductivity and corrosion resistance in oxidizing as well as in a reducing atmospheres. The disadvantages of these materials are poor tolerance to sudden temperature changes and difficulties in producing interconnect with complex shapes.

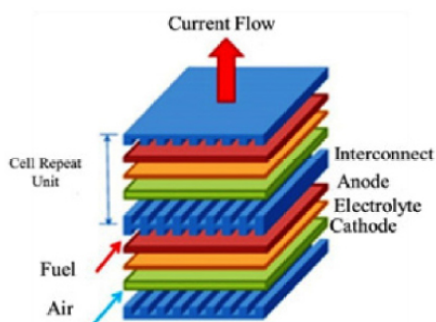


Figure 1. The schematic of SOFC stack [6].

So, the heat-resistant alloys based on nickel, cobalt and iron with an addition of chromium (metallic alloys) may offer an interesting alternative for the ceramic interconnectors [4, 7]. Among metallic alloys, Fe–Cr alloys are suitable for being used as interconnect due to their suitable thermal expansion coefficient, low cost and excellent formability [8-10]. Interconnects should have excellent electrical conductivity and oxidation resistance, good thermal conductivity and thermal expansion coefficient (TEC) matching to those of electrodes and electrolyte [11]. However, particularly in oxidizing atmospheres, the formation of oxide scales leads to high contact resistance which is deleterious to the fuel cell performance [12]. Various coating materials including reactive element oxides (REOs), conductive perovskites,  $\text{MAlCrYO}$  (M represents a metal, e.g., Co, Mn and/or Ti) oxidation resistant systems, conductive spinels and conductive composite spinels have been used in an effort to decrease oxide growth kinetics, increase oxide scale conductivity, and improve oxide scale to metal adhesion [13]. Although different methods such as pulse laser deposition (PLD) has been commonly used to apply  $\text{MnCr}_2\text{O}_4$  protective coating on the surface of metallic interconnects [14], the electrophoretic deposition (EPD) has recently attracted much attention in the application of ceramic layers of different thicknesses. In this

process, ceramic particles dispersed in a liquid medium will migrate under a DC electric field towards the opposite electrode where they finally deposit forming a thick layer on the surface. The EPD technique has advantages such as short formation time, easy control of the layer thickness and morphology along with no needs for complex apparatus [15]. In the present study, the EPD method is employed to deposit  $\text{MnCr}_2\text{O}_4$  spinel particles on SUS 430 SOFC interconnect. At the next step the effect of pre-sintering atmospheres (air and 5%  $\text{H}_2/\text{Ar}$ ) on cyclic oxidation resistance at 800°C for 500h will be investigated.

## 2. Experimental

### 2.1. $\text{MnCr}_2\text{O}_4$ spinel synthesis

$\text{MnCr}_2\text{O}_4$  spinel powder was synthesized by solid state reaction. For synthesis of  $\text{MnCr}_2\text{O}_4$ ,  $\text{MnO}_2$  and  $\text{Cr}_2\text{O}_3$  precursor powders were mixed for 24h in nylon jar using ethanol as the solvent. The slurries were then calcined at 1100°C for 2.5h. The calcined powders were ball-milled in planetary mill for 12h again to obtain the fine powder suitable for EPD. Particle size analysis (PSA) (Fritsch, Germany), in water medium, was used to determine the distribution of synthesized spinel. The XRD technique was employed to characterize the  $\text{MnCr}_2\text{O}_4$  spinel synthesized by solid state reaction. The XRD pattern was recorded (Philips PW3710) using a  $\text{Cu K}_\alpha$  monochromatized radiation source.

### 2.2. EPD and oxidation test

1 gr/L of  $\text{MnCr}_2\text{O}_4$  homogeneous suspension was prepared in acetone by sonicating in an ultrasonic bath (480W @ 35 kHz) for 20min. A high voltage DC power supply (PST1002) was used for deposition of  $\text{MnCr}_2\text{O}_4$  powder on SUS 430 electrodes with  $20 \times 20 \times 3$  (mm\*mm\*mm) dimensions at a distance of 1 cm. The potential range and deposition duration was determined to be 30-300 V/cm and 1min, respectively.

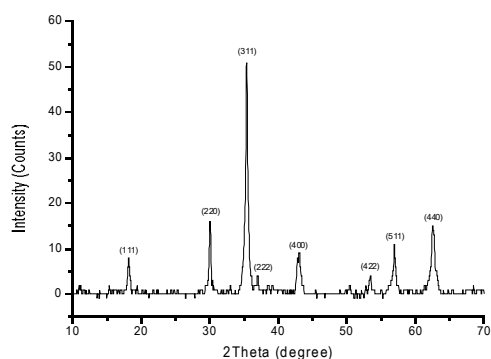
The uncoated and  $\text{MnCr}_2\text{O}_4$  coated SUS 430 samples were pre-sintered in air at 900°C for 3h and then oxidized in air at 800°C for 500h. Also, to study the effect of pre-sintering atmosphere on the oxidation resistance, the pre-sintering of the coated sample was performed in 5%  $\text{H}_2/\text{Ar}$  at 900°C for 3h followed by cyclic oxidation in air at 800°C for 500h in accordance with the operation temperature of SOFC cathode. Each cycle

consisted of 50h of heating in air and then cooling to the room temperature.

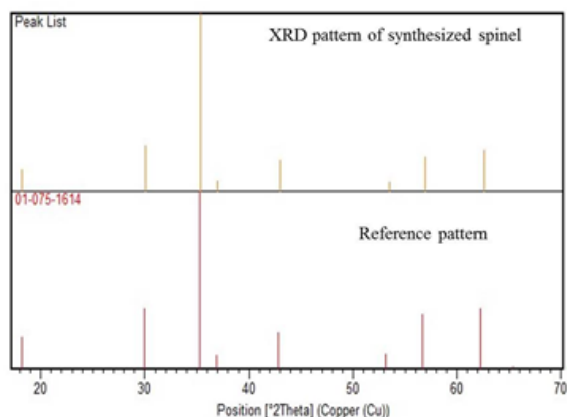
### 3. Result and discussion

#### 3.1. Synthesis of $\text{MnCr}_2\text{O}_4$ spinel

The XRD pattern of synthesized  $\text{MnCr}_2\text{O}_4$  spinel is shown in Figure 2 where all peaks have been identified as  $\text{MnCr}_2\text{O}_4$  powder [JCPDS card number: 01-075-1614]. The particle size distribution of  $\text{MnCr}_2\text{O}_4$  spinel used for EPD is illustrated in Figure 3 where the medium value of the particle size distribution (D50) of the spinel is clearly seen to be 0.875  $\mu\text{m}$ .



(a)



(b)

Figure 2. XRD pattern of synthesized spinel (a) and (b) XRD pattern compared with the reference pattern.

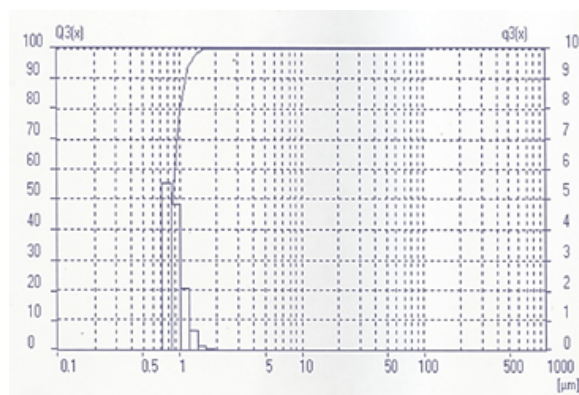


Figure 3. Particle size distribution of  $\text{MnCr}_2\text{O}_4$  spinel powder.

#### 3.2. Effect of electric field on weight deposition

As it was mentioned above, different electric fields were applied for EPD process. Figure 4 shows the weight of deposited  $\text{MnCr}_2\text{O}_4$  on SUS 430 substrate from an acetone based suspension at 30–300 V/cm. The deposition weight is increased as a function of applied electric field because of higher deposition rate of particles. The results are in accordance with the Hamaker Eq [16].

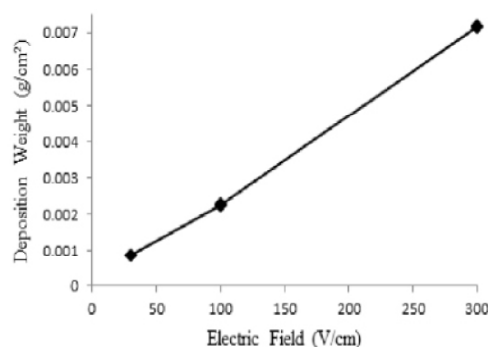


Figure 4. Deposition weight as a function of electric field.

#### 3.3. Effect of electric field on EPD current density

The current density during EPD versus time of deposition for  $\text{MnCr}_2\text{O}_4$  suspension at 30, 100 and 300 V/cm (Figure 5) indicates that the current density decreased with time for all experiments which is attributed to the formation of an insulating layer of  $\text{MnCr}_2\text{O}_4$  particles [15].

As demonstrated in Figure 5, higher voltages resulted in higher current densities which can be attributed to the evident increase in the driving force at higher potentials.

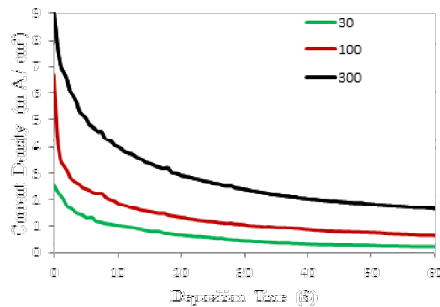


Figure 5. Current density in EPD of  $\text{MnCr}_2\text{O}_4$  at 30 - 300 V/cm.

### 3.4. Oxidation test

The SEM image of specimen coated with  $\text{MnCr}_2\text{O}_4$  spinel coating deposited by EPD at electric field of 300 V/cm is illustrated in Figure 6. The thickness of the uniform and cracked free layer in 300V/cm, measured by the TALY STEP apparatus, was  $\sim 15$  nm.

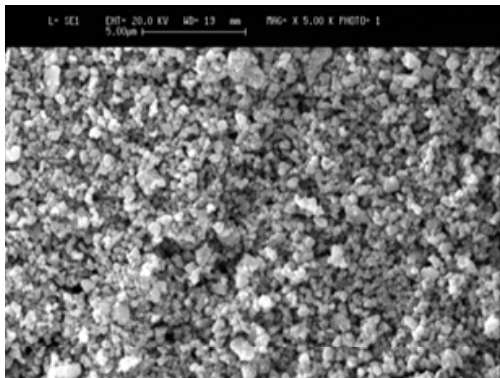


Figure 6. Surface morphology of as deposited  $\text{MnCr}_2\text{O}_4$ .

Coated and uncoated specimens were pre-sintered in air at 900 °C for 3h followed by oxidation at 800 °C for 500h. Figure 7 shows the weight changes of the uncoated and coated specimens as a function of oxidation time during cyclic oxidation test. The squared weight change per area versus oxidation duration (10 cycles) for coated and uncoated specimen revealed that the curves after 50h are linear and obey the Wagner theory based on the following relation (Equation 1):

$$(\Delta W/A)^2 = K_p t \quad (1)$$

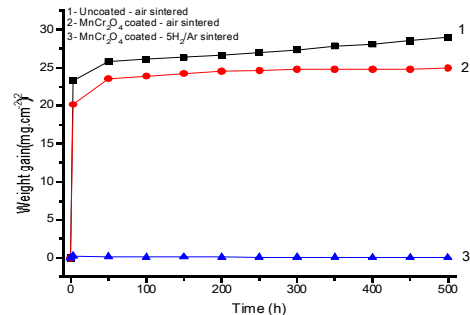


Figure 7. Weight change as a function of oxidation time.

where,  $\Delta W$  is mass gain,  $A$  the surface of coated samples,  $t$  time of oxidation and  $K_p$  the oxidation parabolic rate constant [17]. It is obvious that the weight change of the uncoated specimen was larger than that of the coated one during the cyclic oxidation. Therefore,  $\text{MnCr}_2\text{O}_4$  coating does have a beneficial effect on the oxidation behavior of uncoated steel. In other words, this coating decreased the oxidation rate as compared with the uncoated alloy. The  $K_p$  values for coated and uncoated specimens are listed in Table 1.

Table 1. The oxidation rate constants after 500h oxidation in air at 800°C.

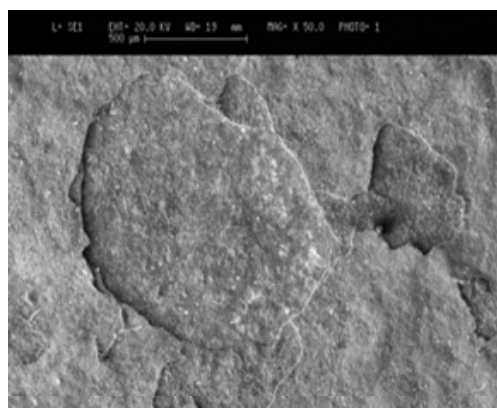
	$K_p(\text{g}^2.\text{cm}^{-4}.\text{s}^{-1})$
Uncoated - air sintered	$1.96 \times 10^{-12}$
$\text{MnCr}_2\text{O}_4$ coated - air sintered	$7.53 \times 10^{-13}$
$\text{MnCr}_2\text{O}_4$ coated - 5H <sub>2</sub> /Ar sintered	$5.25 \times 10^{-14}$

The  $K_p$  for the uncoated specimen was calculated to be  $1.96 \times 10^{-12} \text{ gr}^2.\text{cm}^{-4}.\text{s}^{-1}$ , while for coated pre-sintered specimens in air and 5% H<sub>2</sub>/Ar is  $7.53 \times 10^{-13}$  and  $5.25 \times 10^{-14} \text{ gr}^2.\text{cm}^{-4}.\text{s}^{-1}$ , respectively. It is evident that sintering in hydrogen reducing atmosphere resulted in a 37-fold decrease in the parabolic oxidation rate constant in comparison with the uncoated specimen.

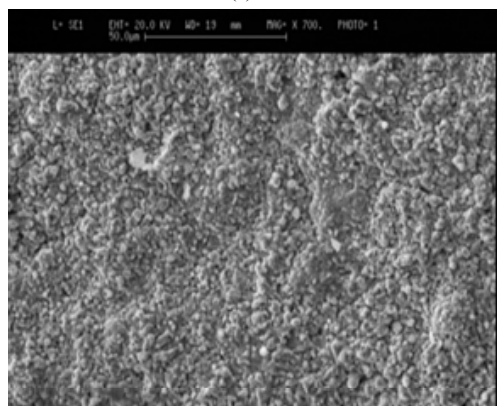
Thus, the coating acted as a barrier for the inward diffusion of the oxygen and effectively reduced the oxidation rate constant. The higher weight change in pre-sintered specimen in reducing atmosphere compared with air pre-sintered specimen can be attributed to the oxygen diffusion from air atmosphere through the oxide layer in the pre-sintering stage.

The surface morphologies of the uncoated and coated samples are shown in Figure 8. As shown

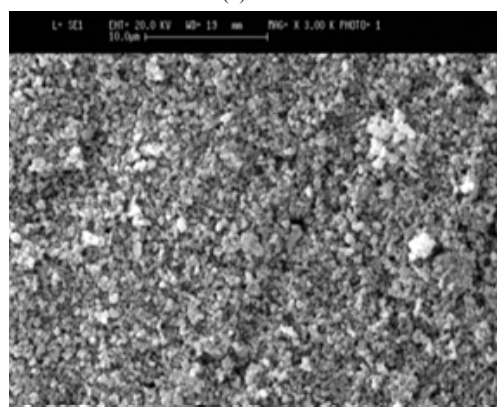
in this Figure, the surface of coated samples was uniform and no spallation was observed. However, spallation areas on the surface of the uncoated samples were visible (Figure 8. a). It is evident that the oxide scale developed on the  $\text{MnCr}_2\text{O}_4$ -coated steel exhibited a higher spallation resistance (see Figure 8.d) than that on the uncoated steel.



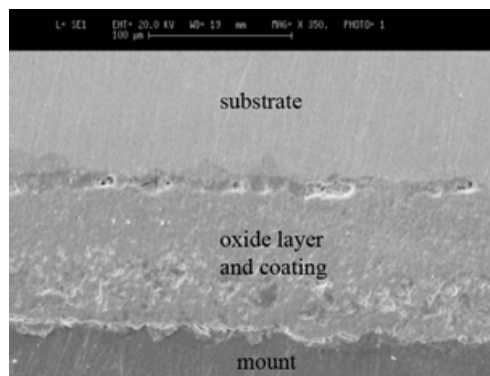
(a)



(b)



(c)



(d)

**Figure 8. SEM surface morphologies of: (a) uncoated sample, (b) coated sample pre sintered in air, (c) coated sample pre sintered in  $5\text{H}_2/\text{Ar}$  after 500h of oxidation at  $800^\circ\text{C}$  and (d) SEM cross section of coated sample pre sintered in air after 500h of oxidation at  $800^\circ\text{C}$ .**

#### 4. Conclusion

The pure  $\text{MnCr}_2\text{O}_4$  spinel with particle size of less than  $1\ \mu\text{m}$  was synthesized by a solid state reaction. The spinel powder was then applied on SUS 430 ferritic stainless steel via EPD. The  $\text{MnCr}_2\text{O}_4$  spinel coating improved the oxidation resistance of SUS 430. The use of a reducing atmosphere before the oxidation of the coated samples had a significant effect on the oxidation behavior decreasing the oxidation rate constant ( $K_p$ ); approximately 37 times compared to the air pre-sintered uncoated sample.

#### 5. References

- [1] Fontana S, Amendola R, Chevalier S, Piccardo P, Caboche G, Viviani M, et al. Metallic interconnects for SOFC: Characterisation of corrosion resistance and conductivity evaluation at operating temperature of differently coated alloys. *Journal of Power Sources*. 2007; 171(2): 652-62.
- [2] Zhu WZ, Deevi SC. Opportunity of metallic interconnects for solid oxide fuel cells: a status on contact resistance. *Materials Research Bulletin*. 2003; 38(6): 957-72.
- [3] Zhu WZ, Deevi SC. Development of interconnect materials for solid oxide fuel cells. *Ma*

- terials Science and Engineering: A. 2003; 348(1–2): 227-43.
- [4] Brylewski T, Nanko M, Maruyama T, Przybylski K. Application of Fe–16Cr ferritic alloy to interconnector for a solid oxide fuel cell. *Solid State Ionics*. 2001, 143(2): 131-50.
- [5] Yoo J, Woo S-K, Yu JH, Lee S, Park GW.  $\text{La}_{0.8}\text{Sr}_{0.2}\text{MnO}_3$  and  $(\text{Mn}_{1.5}\text{Co}_{1.5})\text{O}_4$  double layer coated by electrophoretic deposition on Crofer22 APU for SOEC interconnect applications. *International Journal of Hydrogen Energy*, 2009, 34(3): 1542-7.
- [6] Lai, K., et al. A quasi-two-dimensional electrochemistry modeling tool for planar solid oxide fuel cell stacks. *Journal of Power Sources*, 2011; 196 (6), 3204-3222.
- [7] Yoon KJ, Cramer CN, Stevenson JW, Marina OA. Advanced ceramic interconnect material for solid oxide fuel cells: Electrical and thermal properties of calcium- and nickel-doped yttrium chromites. *Journal of Power Sources*. 2010; 195(22): 7587-93.
- [8] Z. Yang, K.S. Weil, D.M. Paxton, J.W. Stevenson. *J. Electrochem. Soc.* 2003; 150: 1188
- [9] Bateni MR, Wei P, Deng X, Petric A. Spinel coatings for UNS 430 stainless steel interconnects. *Surface and Coatings Technology*. 2007; 201(8): 4677-84.
- [10] Hansson AN, Linderoth S, Mogensen M, Somers MAJ. Inter-diffusion between  $\text{Co}_3\text{O}_4$  coatings and the oxide scale on Fe-22Cr. *Journal of Alloys and Compounds*. 2007; 433(1–2): 193-201.
- [11] Wincewicz KC, Cooper JS. Taxonomies of SOFC material and manufacturing alternatives. *Journal of Power Sources*, 2005, 140(2): 280-96.
- [12] Chen X, Hou PY, Jacobson CP, Visco SJ, De Jonghe LC. Protective coating on stainless steel interconnect for SOFCs: oxidation kinetics and electrical properties. *Solid State Ionics*. 2005; 176(5–6): 425-33.
- [13] Shaigan N, Qu W, Ivey DG, Chen W. A review of recent progress in coatings, surface modifications and alloy developments for solid oxide fuel cell ferritic stainless steel interconnects. *Journal of Power Sources*. 2010, 195(6): 1529-42.
- [14] Mikkelsen L, Chen M, Hendriksen PV, Persson A, Pryds N, Rodrigo K. Deposition of  $\text{La}_{0.8}\text{Sr}_{0.2}\text{Cr}_{0.97}\text{V}_{0.03}\text{O}_3$  and  $\text{MnCr}_2\text{O}_4$  thin films on ferritic alloy for solid oxide fuel cell application. *Surface and Coatings Technology*. 2007, 202(4–7): 1262-6.
- [15] Laxmidhar Besra, Meilin Liu. A review on fundamentals and applications of electrophoretic deposition (EPD). *Progress in Materials Science*, 2007, 52(1): 1-61.
- [16] Hamaker HC. Formation of deposition by electrophoresis. *Trans Farad Soc* 1940; 36: 279–83.
- [17] C. Wagner, *Z. Phys. Chem. B21*. 1933: 42.